

## Comparison of Conformational Analysis Techniques To Generate Pharmacophore Hypotheses Using Catalyst

Rajendra Kristam,<sup>†,§</sup> Valerie J. Gillet,<sup>\*,†</sup> Richard A. Lewis,<sup>‡,||</sup> and David Thorner<sup>‡</sup>

Department of Information Studies, University of Sheffield, Regent Court, 211 Portobello Street, Sheffield S1 4DP, U.K., and Eli Lilly & Co., Windlesham GU20 6PH, Surrey, U.K.

Received August 31, 2004

Generation of reliable pharmacophore models is a key strategy in drug design. The quality of a pharmacophore model is known to depend on several factors, with the quality of the conformer sets used perhaps being one of the most important. The goal of this study was to compare different conformational analysis methods to determine if one was superior to the others for pharmacophore generation using Catalyst/HypoGen. The five methods selected were Catalyst/Fast, Catalyst/Best, Omega, Chem-X and MacroModel. Data sets for which Catalysts models had previously been published were selected using defined quality measures. Hypotheses were generated for each of the data sets and the performance of the different conformational analysis methods was compared using both quantitative (cost and correlation coefficients) and qualitative measures (by comparing the hypotheses in terms of the features present and their spatial relationships). Two main conclusions emerged from the study. First, it was not always possible to replicate the literature results. The reasons for these failures are explored in detail, and a template for use in publications that apply the Catalyst methodology is proposed. Second, the faster rule-based methods for conformational analysis give pharmacophore models that are just as good as, and in some cases better than, the models generated using the slower, more rigorous approaches.

### INTRODUCTION

A pharmacophore is defined as the set of chemical features and the spatial relationships between these features that together form a necessary requirement for biological activity.<sup>1</sup> A pharmacophore can help medicinal chemists visualize the potential interactions between the ligand and receptor; it can be used as a query in a 3D database search to identify new structural classes of potential lead compounds; and it can serve as a template for generating alignments for 3D-QSAR analysis.<sup>2</sup> Thus, the construction of an accurate pharmacophore is a key objective in many drug discovery efforts.

Pharmacophore identification is now increasingly being handled by automated computational methods, for example, Catalyst, GASP and DISCO are three commercially available programs.<sup>3–5</sup> We focus on Catalyst<sup>6</sup> in this paper. The Catalyst program operates in two modes: HipHop and HypoGen. Catalyst/HipHop generates pharmacophore hypotheses using active compounds only. Catalyst/HypoGen takes activity data into account and uses both active and inactive compounds in an attempt to identify hypotheses that are common among the active compounds but not among the inactives. HypoGen builds hypotheses in three steps: a constructive step, a subtractive step and an optimization step. The constructive step identifies pharmacophore candidates

that are present in the most active set of compounds. The subtractive phase then eliminates configurations that are also present in at least half of the inactive compounds. The final optimization step attempts to improve the score of the remaining hypotheses by applying small perturbations. HypoGen, thus, attempts to build hypotheses or SARs that correlate estimated activities with experimental activities and that can be used subsequently to predict the activities of new compounds. The hypotheses can also be used in database searching.

The two major issues in pharmacophore identification are the correct representation of the chemical features, so that bioequivalent features are mapped together, and the appropriate sampling of conformation space so that the bioactive conformation of each compound is found.<sup>7,8</sup> In Catalyst, pharmacophores are described in terms of features such as hydrogen bond-donors (HBD), acceptors (HBA), hydrophobic regions, and charged centers with the default definitions of the features being customizable.<sup>9</sup> A maximum of five types of features can be specified. Features that have directionality (HBD, HBA, aromatic hydrophobic features) are described using two points with a single point being used to describe nondirectional features (charged centers, aliphatic hydrophobic regions).

Ensuring that the bioactive conformations of the compounds are sampled is a major challenge since, in most cases, the precise form of the bioactive conformation is not known experimentally and most compounds can exist in a large number of conformations. The bioactive conformation does not always correspond to an energy minimum of the ligand in its unbound form. We make the assumption that ligands with strong affinity for their receptor are not having to

\* Corresponding author fax: +44 1142 780 300; e-mail: v.gillet@sheffield.ac.uk.

<sup>†</sup> University of Sheffield.

<sup>‡</sup> Eli Lilly & Co.

<sup>§</sup> Current address: Aurigene Discovery Technologies Limited, 39-40, KIADB Industrial Area, Electronic City Phase II, Hosur Road, Bangalore 560 100, India.

<sup>||</sup> Current address: WKL-136.3.94, Novartis Pharma AG, CH-4002 Basel, Switzerland.

**Table 1.** Data Sets<sup>a</sup>

set no.	publication	no. of compounds (training set)	energy threshold (kcal/mol)	no. of conformations	CA program used (as mentioned in the paper)
1	Bureau et al. <sup>13</sup>	15	20	250	not specified
2	Barbaro et al. <sup>14</sup>	24	20	250	Catalyst/Best assumed
3	Kim et al. <sup>15</sup>	21	10	250	Catalyst/Best
4	Debnath <sup>16</sup>	20	20	250	not specified
5	Debnath <sup>16</sup>	20	20	250	Catalyst/Best assumed
6	Ekins et al. <sup>17</sup>	16	20	255	Catalyst/Best

<sup>a</sup> The number of compounds in each training set, the energy threshold used, the maximum limit for the number of conformations and the conformational technique used.

**Table 2.** Catalyst Parameters as Specified in the Publications Including the Chemical Features Set, the Uncertainty Value Used, Constraints Set, if Any, and the Assumptions Made, if Any<sup>a</sup>

set no.	chemical features specified	uncertainty value	constraints, if any	assumptions
1	HBA, HPh, PI, RA	3		
2	HBAI, HBD, HPh, PI, RA	3	1. hypotheses should have five features 2. PI to be present in all hypotheses	uncertainty value
3	HBA, HBD, HPh	3	1. hypotheses should have four features	uncertainty value
4	HBA, HBD, HPh, RA	3		
5	HBA, HBD, HPh, RA	3		
6	HBA, HBD, HPh, RA	3		uncertainty value

<sup>a</sup> The chemical features are as follows: HBA – Hydrogen Bond Acceptor; HPh – Hydrophobic; HBD – Hydrogen Bond Donor; PI – Positive Ionisable; HBAI – Hydrogen Bond Acceptor Lipid; RA – Ring Aromatic. The uncertainty value denotes the range of uncertainty in the activity value—an uncertainty value of 3 (default) in the biological activity means that it is located somewhere in the range “activity/3” to “activity\*3”.

channel much energy into accessing a high energy conformation. The problem of conformational flexibility is addressed in Catalyst by performing conformational analysis prior to hypothesis generation and considering each conformer of each compound in turn.

Many different conformational analysis programs have been developed using a variety of different computational techniques.<sup>10</sup> In two recent studies, Boström and colleagues compared various methods on their ability to reproduce bioactive conformations as determined from high quality X-ray protein–ligand complexes.<sup>7,11</sup> In this paper, we compare five conformational analysis methods, namely Catalyst/Fast, Catalyst/Best, Chem-X, Omega and Macro-Model, by examining the pharmacophore hypotheses generated using Catalyst/Hypogen. Literature data sets were chosen using well-defined criteria. Hypotheses were generated using each of the conformer sets and were compared quantitatively, based on correlations between observed and predicted activities, and qualitatively, to see if the literature models were reproduced and to examine the consistency of the hypotheses across the different methods.

## METHODS

Six high quality data sets were selected from peer-reviewed journals using the following criteria: the pharmacophore models should have been produced in Catalyst using its Hypogen module; sufficient data (structure drawings, parameters used in the experiment, and conditions for the experiment) should have been specified to repeat the experiment; the training set should preferably have been selected following the Catalyst picking rules;<sup>12</sup> there should be 15–25 compounds to ensure sufficient training of Catalyst.

The publications from which the data sets were extracted are shown in Table 1, and the compounds together with their

activity values are given in the Supporting Information.<sup>13–17</sup> Sets 1, 2 and 6 represent fairly diverse compound sets, whereas Sets 3, 4 and 5 consist of structurally similar compounds.

The structures were redrawn and converted into 3D structures using Corina.<sup>18</sup> For each data set, five conformer sets were generated using the five conformational analysis (CA) methods (details below) giving a total of 30 conformational sets. Wherever specified, the stereochemistry (chirality) of the compounds in each data set was fixed in the input files. In some data sets, the stereochemistry was not given for some compounds (Set 1), while in other data sets it was not given for any compounds (Set 6). In these cases, the stereochemistry was left as unspecified, and Catalyst was allowed to set it. Usually in such cases Catalyst fixes the stereochemistry as ‘unknown’. Hypogen has a limit of 250 conformers per structure, so the analyses were tailored to this limit.

The output from each CA program was imported into HypoGen, and hypotheses were generated for each data set. Activity values, uncertainty values and chemical features were set to the values given in the original publications. The parameters used and any assumptions made to produce the hypotheses for each data set are summarized in Table 2. In the cases of Sets 2, 3 and 6, the uncertainty values were assumed to be the default value of 3. All other parameters were set at default values unless otherwise specified in the publications.

HypoGen ranks the hypotheses on their cost value; this consists of three components, namely, the weight cost, the error cost and the configuration cost. The weight component increases in a Gaussian form as the feature weight deviates from the idealized value of 2.0. The error cost increases as the RMS distance between the estimated and the measured

activities for the training set increases. The configuration cost represents the complexity or the entropy of the hypothesis space being optimized and is constant for a given data set.

Catalyst first calculates the costs of two theoretical hypotheses, namely, the ideal hypothesis (fixed cost) and the null hypothesis. The ideal hypothesis has a minimal error cost, and the slope of the activity correlation is one. The null hypothesis has a maximal error cost, and the slope of the activity correlation is zero. Together they represent the upper and lower bounds on cost for the hypotheses that are generated. The greater the difference between them, the greater is the likelihood that a meaningful hypothesis can be found. The closer the cost of the generated hypothesis is to that of the ideal hypothesis, the higher the probability that the generated hypothesis represents a true correlation in the data. The hypothesis with the least cost ideally would map to all the features of the most active compounds in the training set. The cost is reported in bits and a difference of about 50–60 bits between the generated hypotheses and the null hypothesis suggests that the correlation may be significant which in turn requires a difference of about 60–70 bits between the costs of the ideal and null hypotheses.

Three correlation coefficients were also used to evaluate the hypotheses: the Catalyst correlation score, Pearson's correlation coefficient and Spearman's rank correlation coefficient. The Catalyst correlation score is derived from the simple linear regression between the experimental and the estimated activities. The correlation coefficient can range from  $-1$  to  $+1$ , with positive values indicating a direct linear relationship between the two variables, i.e., the experimental and estimated values. Pearson's correlation coefficient indicates the degree of covariation of two variables and was used to compare the estimated values with the experimental values. The closer they are, the better the correlation. Spearman's correlation coefficient measures the relationship between the relative ranks of the estimated and experimental values.

#### CONFORMATIONAL ANALYSIS METHODS

All of the literature data sets use either Catalyst/Fast, Catalyst/Best or the conformational analysis tool was not specified, in which case it has been assumed that either Fast or Best was used. The various parameters used to generate the conformations in the original publications are summarized in Table 1. The methods and the parameter settings used here are described briefly below.

**Catalyst/Fast and Catalyst/Best.** Catalyst incorporates two methods of conformational model generation, namely, Best and Fast.<sup>19</sup> Both use a version of the CHARMM force field for energy calculations and a poling mechanism for forcing the search into unexplored regions of conformer space.<sup>20</sup> Best searches the conformational space more extensively than Fast, particularly ring conformations, and it applies more stringent minimization procedures. Fast is more approximate and therefore requires substantially less computational time. For Fast and Best, 250 conformers were requested for each compound in each set. The other parameters were left at their default settings, and an energy threshold of 20 kcal/mol was used, except for Set 3 where the threshold was 10 kcal/mol.

**Chem-X.** Chem-X is a rule-based conformational analysis program. It was used with the corrections described by

Mason et al. for crowded  $sp^2$  systems<sup>21</sup> and with an energy cutoff of 20 kcal/mol. Unreasonable structures are avoided by a 'bump check' that eliminates structures with contacts closer than 3/5 vdW radii. The default samplings of 3 rotamers for single bonds, 6 for  $sp^2$ - $sp^3$  bonds, 2 for double and conjugated bonds and a limit of up to 10 rotatable bonds were used. The output is ranked on energy, and where the number of conformations exceeded 250, the top ranking 250 were chosen.

**Omega.** Omega is a deterministic rule-based method for conformer searching in which rotatable bonds are automatically perceived and a user-specified or default torsion is applied to them.<sup>22</sup> Omega does not optimize the input bond lengths, bond angles and ring conformations in the assembly step, and it lacks an explicit term in the conformational energy to account for variations in these parameters. The conformations of ring systems are taken from a ring library file by default. The energy window and the maximum number of conformations are user-definable and limit the final number of conformations. Omega uses the Clean force field for energy. Duplicate conformers are detected by calculating the root-mean-square distances between the heavy atoms. Omega was run using default settings, and any protonation states set by Omega were returned to their neutral form before use in Catalyst.

**MacroModel.** MacroModel<sup>23</sup> was used in its MCMM (MacroModel Monte Carlo Multiple Minimum) mode of conformational search in which a Monte Carlo method is used to modify the input structures by random changes in the torsion angles and/or molecular positions. Rings are handled by selecting the ring closure atoms distances and angles, breaking the ring bond, performing the Monte Carlo torsion angle searching and reassembling the ring. The chirality of the starting structure is maintained. The MMFF force field in MacroModel 8.0 was used for energy calculation. MacroModel was run in "perform automatic setup" mode. The energy threshold and the number of steps were set to 20 kcal/mol and 1000, respectively. These values were chosen following an investigation of the relationship between the number of rotatable bonds and the conformers produced. If the number of conformations exceeded 250, the number of steps was reduced, and the analysis was repeated.

All the conformational analysis studies were carried out on a Silicon Graphics Origin200 workstation running IRIX 6.5.1 using the following program versions: Chem-X (version Jan 2000), Omega (v1.0b9), MacroModel 8.1 and Catalyst 4.7 (ConFirm). All the pharmacophore models were built using Catalyst/HypoGen version 4.7 (catHypo).

#### RESULTS

The hypotheses generated using the different conformational analysis methods were evaluated by examining the cost values of the hypotheses; by calculating the three correlation coefficients identified above; and by qualitatively comparing the hypotheses generated. The latter comparison was derived from the expectation that the literature results would be reproducible and that the study would demonstrate whether a different conformer set would generate superior results. This comparison would also allow the consistency of the hypotheses generated using different conformational analysis methods to be investigated. Unless otherwise



**Table 3.** Correlation Coefficient Values and Costs Obtained for Set 1

	literature	Fast	Best	Chem-X	Omega	MacroModel
Catalyst score		0.892	0.964	0.978	0.942	0.955
Pearson	0.925 <sup>a</sup>	0.944	0.629	0.904	0.79	0.742
Spearman	0.907 <sup>a</sup>	0.868	0.946	0.982	0.95	0.954
ideal cost	75	68.34	69.15	67.24	69.01	68.54
null cost	150.4	129.85	129.85	129.85	129.85	129.85
hypothesis cost		85.02	76.14	72.13	80.03	76.29

<sup>a</sup> Values calculated from data presented in ref 13.**Table 4.** Summary of the Chemical Features in the Hypotheses Generated for Set 1

	features
Fast	3 HPh, 2 RA
Best	2 HPh, 1 RA, 1 PI, 1HBA
Chem-X	2 HPh, 1 RA, 1 PI, 1HBA
Omega	2 HPh, 1 PI, 2 HBA
MacroModel	3 HPh, 2 HBA
literature	2 HPh, 1 RA, 1 PI, 1 HBA

indicated, results are presented for the top ranking hypothesis only.

**Set 1.** The correlation scores and costs for the top scoring hypothesis for each conformational analysis method are reported in Table 3 together with the results for the literature hypothesis which have been calculated from data presented in the publication. It can be seen that the scores are similar to those for the literature model. All the conformational analysis programs gave very good Catalyst and Spearman's scores and, comparatively, slightly lower Pearson's scores. Chem-X also gave a good Pearson's score and gave the best results overall, while Fast gave comparatively lower results.

The plots of experimental versus estimated activity values are shown in Figure 1. The plots obtained for Best, Chem-X and MacroModel are all excellent, with most of the predicted values falling within half a log unit of the actual value. Only one compound falls outside this error range for the Best hypothesis and two for the MacroModel hypothesis. In the case of Chem-X, all of the structures predict within the error range. Both the Fast and Omega plots show clustering, due to poor fitting of certain structural features to the hypotheses.

The costs associated with the top ranking hypotheses are given in Table 3. The difference between the ideal and null costs is about 60 bits and that between the hypotheses and null hypotheses is in the range 45–58. It can be seen that Chem-X gives a lower ideal cost and hypothesis cost which correspond with the better correlation scores seen, especially Pearson's coefficient. Fast gives higher costs and correspondingly lower correlation values.

On inspection of the hypotheses, however, none of the top ranked hypotheses looked similar to that reported in the literature with respect to the number and type of chemical features. In the publication, additional criteria, external to the Catalyst method, were applied to select the "best" model from the top 10 models, and it is not clear which of the 10 models is reported. Thus, for this data set, the top 10 scoring hypotheses were examined visually in each case, and the one that seemed closest to the literature "best" hypothesis was selected for the qualitative comparison. The features present in each hypothesis are shown in Table 4.

Compound 8 of the data set is illustrated in Figure 2, and the mappings of the hypotheses onto it are shown in Figure

3. The literature hypothesis has the RA mapped to the benzene ring, the two HPhs are mapped to the chlorine substituent and the butyl group of the piperidine, respectively, the HBA maps to the carbonyl oxygen and the PI maps to the piperidine nitrogen. The Fast hypothesis (hypothesis at rank 5) has the RA mapped to the benzene ring and the two HPhs mapped to the chlorine substituent and the butyl chain as in the literature hypothesis, but the additional HPh is mapped to the methylene groups of the piperidine group and the other RA is not mapped at all. The Best hypothesis (hypothesis at rank 4) maps all the features as for the literature hypothesis. The Chem-X hypothesis (hypothesis at rank 5) has the PI, HBA and one HPh group mapped as in the literature model, but the RA does not map to anything and the other HPh is mapped to methylene groups of the dioxine moiety. The Omega hypothesis (hypothesis at rank 5) has the PI, one of the HPhs and one of the HBA features mapped as in the literature hypothesis, but the other HPh maps onto the methylene groups of the dioxine moiety and the second HBA does not map to anything. The MacroModel hypothesis (hypothesis at rank 1) has the three HPh features mapped to the butyl chain and the methylene groups of the piperidine and dioxine groups, respectively.

In summary, Chem-X gave the best overall results based on the statistical measures. However, none of the top scoring hypotheses matched the literature hypothesis. The fourth ranked Best hypothesis did match the published model and has similar (but not identical) correlation scores. The Chem-X hypothesis that is closest to the literature model has the same features but the mapping onto compound 8 is different. Both MacroModel and Fast miss the PI feature and Omega exchanges an HBA for a Hydrophobic feature compared to the literature model. The only feature substitution which is permissible is the substitution of a RA with a Hydrophobe, although even in this case there is a loss of specificity.

**Set 2.** The correlation scores and costs for the top scoring hypotheses are reported in Table 5 together with the results in the original publication (either given or calculated from data present therein). All scores are worse than those reported for the literature model. Pearson's coefficient, in particular, is low for most hypotheses implying that they would estimate the experimental activities poorly.

The plots of experimental versus estimated activities for each program are shown in Figure 4. Chem-X and Best produce the best plots, while Omega and MacroModel produce the worst. In the case of Omega, twelve out of the twenty-four compounds have predicted values that fall outside of the error range. For MacroModel, several of the predicted values are equivalent due to poor fitting of the hypothesis to the selected conformers, indicating that at least one feature fails to map to the hypothesis. Thus, the

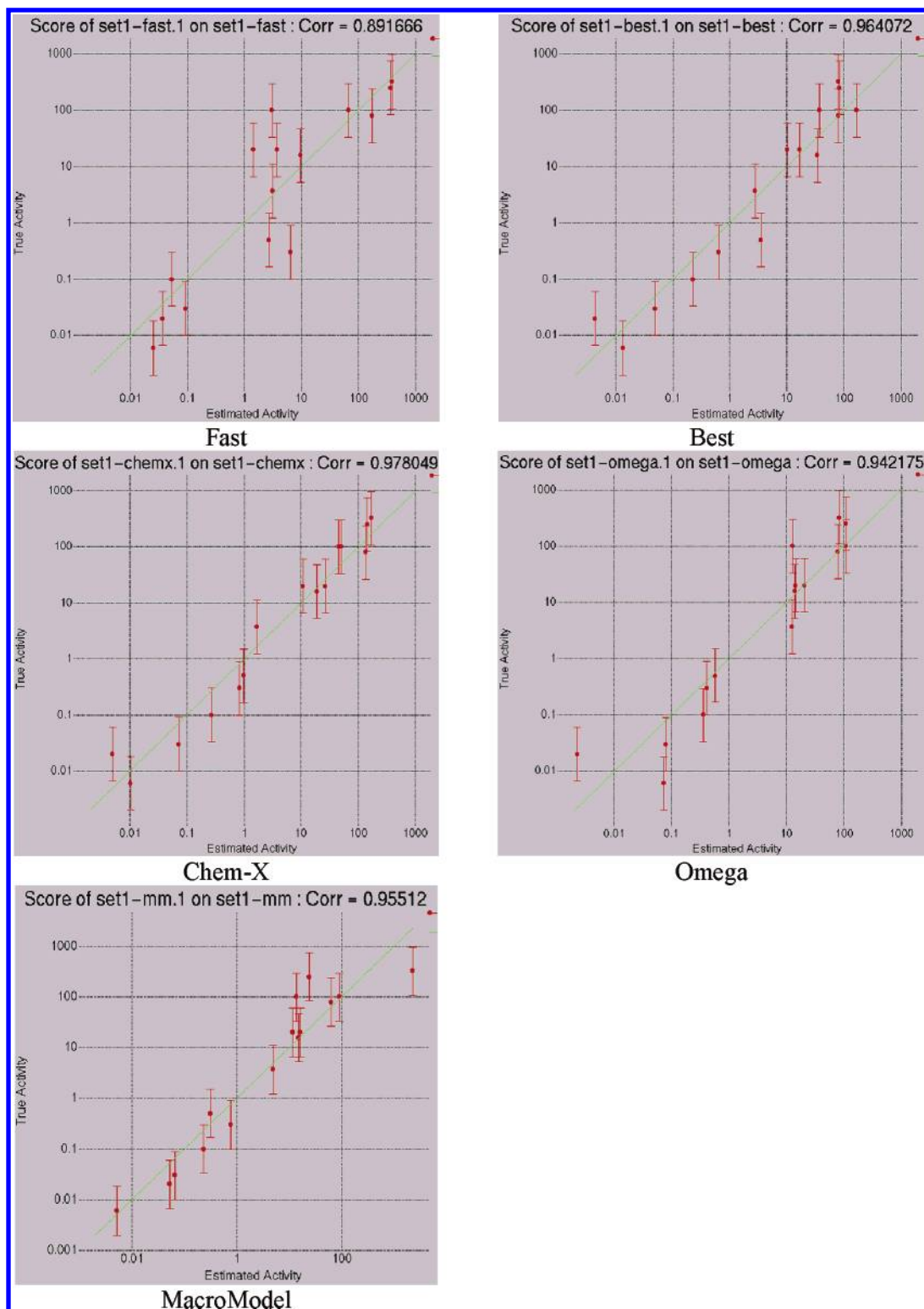


**Figure 1.** Predicted versus experimental values plots for the hypotheses generated for Set 1.

hypothesis generated using MacroModel is of poorer quality than the hypotheses generated from the other conformational analyses methods.

The costs of the hypotheses are given in Table 5. Not surprisingly, Chem-X has the lowest cost and the smallest difference between its ideal cost and the hypothesis cost at 15.90, with the difference between the hypothesis cost and the null cost being 38.08. MacroModel has the largest difference between the hypothesis cost and the ideal cost of all methods at 27.07, and this is larger than the difference

between the null cost and the hypothesis cost and indicates that the hypothesis is not statistically valid. None of the costs agree with the literature costs.

Table 6 lists the features found in each hypothesis. The Best and Omega hypotheses consist of the same features as the literature hypothesis; however, in both cases the spatial arrangement of the features differs from the literature model. This is illustrated in Figure 6 which shows the mappings of the hypotheses onto compound 1, Figure 5. The hypotheses generated using the other programs all differ from the

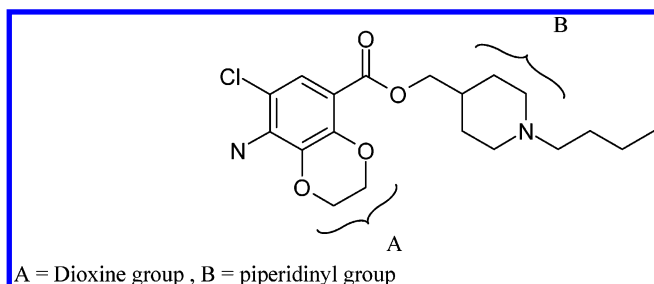


**Figure 2.** Compound 8 of Set 2.

literature hypothesis in the features identified and there is little consistency between them. The mappings of the hypotheses to compounds 1 and 15 are summarized in Table 7 and are described below.

**Mappings to Compound 1.** The literature hypothesis has the HBA mapped to the carbonyl oxygen of pyridazine C, the PI is mapped to a nitrogen of the piperazine D and the three HPhs are mapped to the benzene ring E, its methoxy substituent and the methylene groups of piperazine B, respectively. The Fast hypothesis has two HPhs mapped to the methoxy group of benzene E and the methylene groups of piperazine B, respectively, and the PI is mapped to the nitrogen of piperazine D as for the literature model. The RA is mapped to benzene E, instead of the HPh group in the literature hypotheses. The HBD feature is not mapped to anything in compound 1. The Best hypothesis has two of the three HPhs mapped to benzene E and the methylene groups of piperazine B, respectively, the PI is mapped to a nitrogen of piperazine D and the HBA is mapped to the carbonyl oxygen of pyridazine C as for the literature model. The third HPh is missing. The Chem-X hypothesis has two HPhs mapped to piperazine B and the methoxy group of benzene E, respectively. The PI is mapped to a nitrogen of piperazine D, and the HBA is mapped to the carbonyl oxygen of pyridazine C. Both the Omega and MacroModel hypotheses have three HPhs mapped to benzene ring E, its methoxy substituent and piperazine group B, and the PI is mapped to a nitrogen of piperazine D as for the literature model. In the Omega hypothesis the HBA is not mapped to anything, and the HBD feature in the MacroModel hypothesis is not mapped to anything.

**Mappings to Compound 15.** The literature hypothesis has the HBA mapped to the 1-carbonyl oxygen of the dione (on ring C), the three HPhs are mapped to benzene A, benzene E and its methoxy substituent and the PI is mapped to the 2-nitrogen of piperazine D. The Fast hypothesis has two HPhs mapped to benzene A and the methoxy substituent of benzene E, respectively, the RA is mapped to benzene E, the PI is mapped to the 2-nitrogen of piperazine D and the HBD is mapped to one of the nitrogens of C. The Best hypothesis maps all the features as for the literature hypothesis. The Chem-X hypothesis is the same as the literature hypothesis except that the HPh mapped to benzene E in the literature model is replaced by an RA feature. The mapping of all the features in the Omega hypothesis is the same as the literature hypothesis. The MacroModel hypothesis has the same mapping of features as the Fast hypothesis except that a HPh feature replaces the RA of the Fast hypothesis.

In summary, in terms of correlation scores, Chem-X and Best show the best performance with both MacroModel and Omega showing poor correlations of estimated versus experimental activities. The qualitative comparison revealed that only the Best and Omega hypotheses consist of the same features as the literature model; however, in both cases the spatial arrangement of the features is different. The Fast and MacroModel hypotheses both exchange a HBD feature for HBA.

**Set 3.** The Catalyst scores for the hypotheses produced for Set 3 are close to, but not better than, those reported in the literature, Table 8. (The predicted scores were not given in the publication, hence Pearson's and Spearman's scores were not available for the literature hypothesis). The Catalyst scores and Spearman's coefficients were slightly better than the Pearson's coefficients. MacroModel gave low scores overall although the difference is slight.

The difference between the ideal and null costs is about 80 bits and that between the null hypotheses and the generated hypotheses is about 47–58 bits. Chem-X and Best give overall lower costs and MacroModel gives higher costs. The trend corresponds to that seen in the correlation scores. The costs are slightly higher than those reported in the literature.

The summary of features in the hypotheses is shown in Table 9 where it can be seen that the number and type of features for each hypothesis generated is the same as in the literature hypothesis except for the Best hypothesis; however, the spatial arrangement of the features is different for each hypothesis.

The mappings of the hypotheses to compound 13 (Figure 7) are shown in Figure 8 and are summarized in Table 10.

The literature hypothesis has the three HBAs mapped to the sulfur of the thiazole, the carbonyl oxygen and the nitrogen of the quinazolinyl group, respectively. The HPh is mapped to the phenyl moiety of the quinazolinyl group. The Fast hypothesis has all the features mapped the same as the literature hypothesis except that one of the HBAs is mapped to one of the carbonyl oxygens of the pentanedioic acid rather than the sulfur of the thiazole group. The Best hypothesis has two HBAs mapped to the carbonyl oxygen of the quinazolinyl group and the sulfur of the thiazole group, as in the literature hypothesis. The HPhs are mapped to the phenyl moiety and the methyl substituent of the quinazolinyl group. The Chem-X hypothesis has two HBAs mapped to the sulfur of the thiazole group and the carbonyl of the quinazolinyl group, and the HPh is mapped to the phenyl moiety of the quinazolinyl group, as in the literature hypothesis. The remaining HBA is mapped to the 1-carbonyl group of the pentanedioic acid. The Omega hypothesis has two of the three HBAs mapped to the sulfur of the thiazole group and the carbonyl moiety of the carbonyl amino group, and the other HBA is not mapped to anything. The HPh is mapped to the methyl substituent of the quinazolinyl group. The MacroModel hypothesis has HBAs mapped to the carbonyl group of the quinazolinyl group and the nitrogen of the quinazolinyl group, and the HPh is mapped to the phenyl moiety of the quinazolinyl group, as for the literature hypothesis. The remaining HBA is mapped to the 5-carbonyl group of the pentanedioic acid.

In summary, Best and Chem-X produced the best correlation scores taking all three scores into account. All of



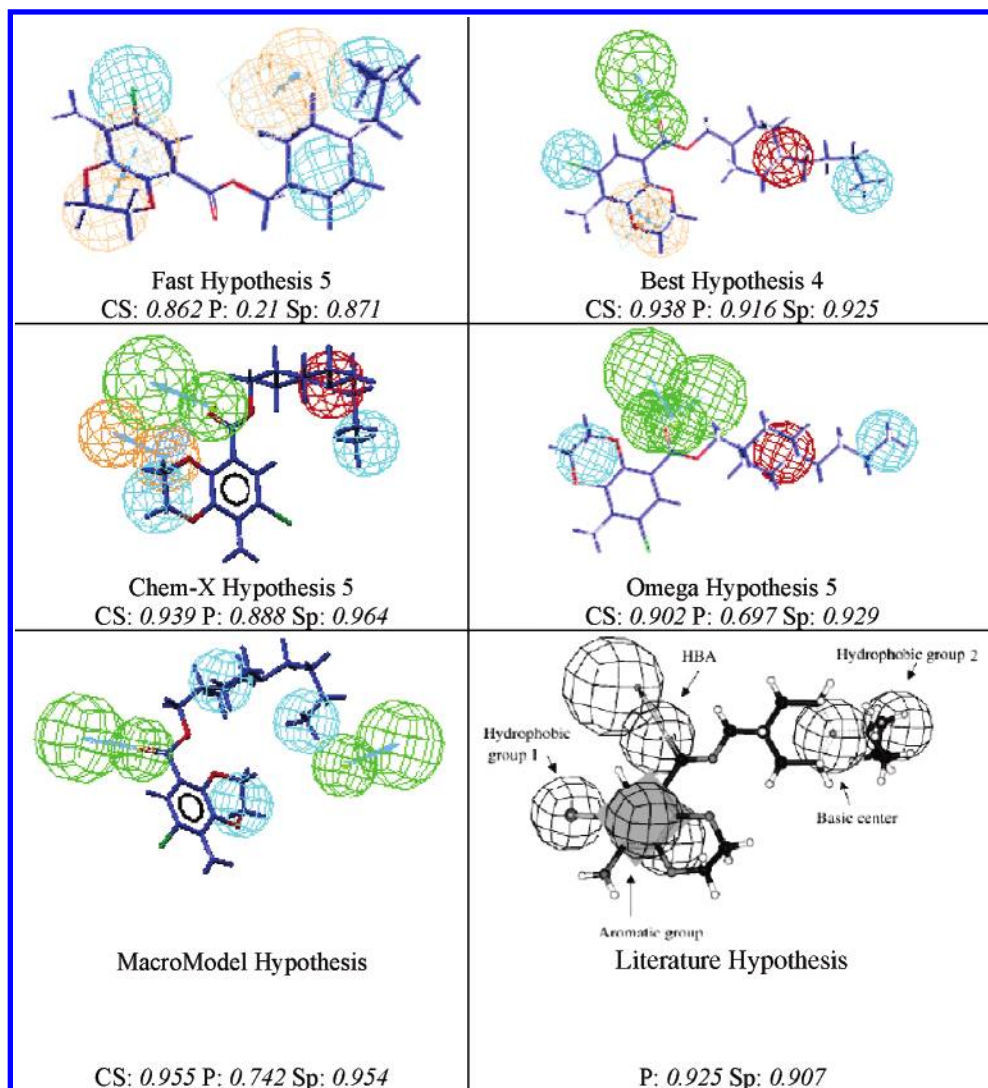


**Figure 3.** Compound 8 of Set 1 mapped onto the ‘best’ hypothesis for each program. The bottom right hand figure is reproduced from the literature showing the mapping of compound 8 onto the best hypothesis selected by the authors. The three correlation scores for the respective hypothesis are also given under each figure. CS=Catalyst Score; P=Pearson’s coefficient; Sp=Spearman’s coefficient. [Reproduced with permission from *J. Chem. Inf. Comput. Sci.* **2002**, 42, 962–967. Copyright 2002 American Chemical Society.]

**Table 5.** Correlation Coefficient Values and Costs Obtained for Set 2

	literature (Best)	Fast	Best	Chem-X	Omega	MacroModel
Catalyst score	0.92	0.807	0.851	0.888	0.782	0.779
Pearson	0.96 <sup>a</sup>	0.477	0.755	0.622	0.921	0.708
Spearman	0.93 <sup>a</sup>	0.764	0.876	0.897	0.753	0.639
ideal cost	100.9	91.77	95.1	93.43	93.67	95.40
null cost	154.9	148.13	148.13	148.13	148.13	148.13
hypothesis cost	112.9	116.17	114.64	109.33	120.34	122.47

<sup>a</sup> Values calculated from data presented in ref 14.

the hypotheses agree with the literature hypothesis, in terms of the number and type of features, except the Best hypothesis; however, the spatial arrangement of the features is different in each case as is the mapping of the features to compound 13.

**Set 4.** All the programs produced hypotheses with Catalyst and Spearman scores that are close to, or better than, those reported in the literature. Chem-X and Best also have good Pearson’s scores with the other methods showing slightly lower scores for Pearson’s coefficient, Table 11. Chem-X has the lowest Catalyst score of all methods, although it is still close to the literature score.

In all cases, the difference between the ideal and null costs is about 60 bits and between the null hypothesis and the generated hypotheses is about 48–54 bits. Thus the costs suggest that the hypotheses are valid, and they further support the high correlation scores seen for all the CA sets. The costs are close to those reported in the literature.

The features present in each of the hypotheses are summarized in Table 12. The mappings of the hypotheses onto compound 1 (Figure 9), the most active compound, are shown in Figure 10, and a summary of the mappings is given in Table 13.

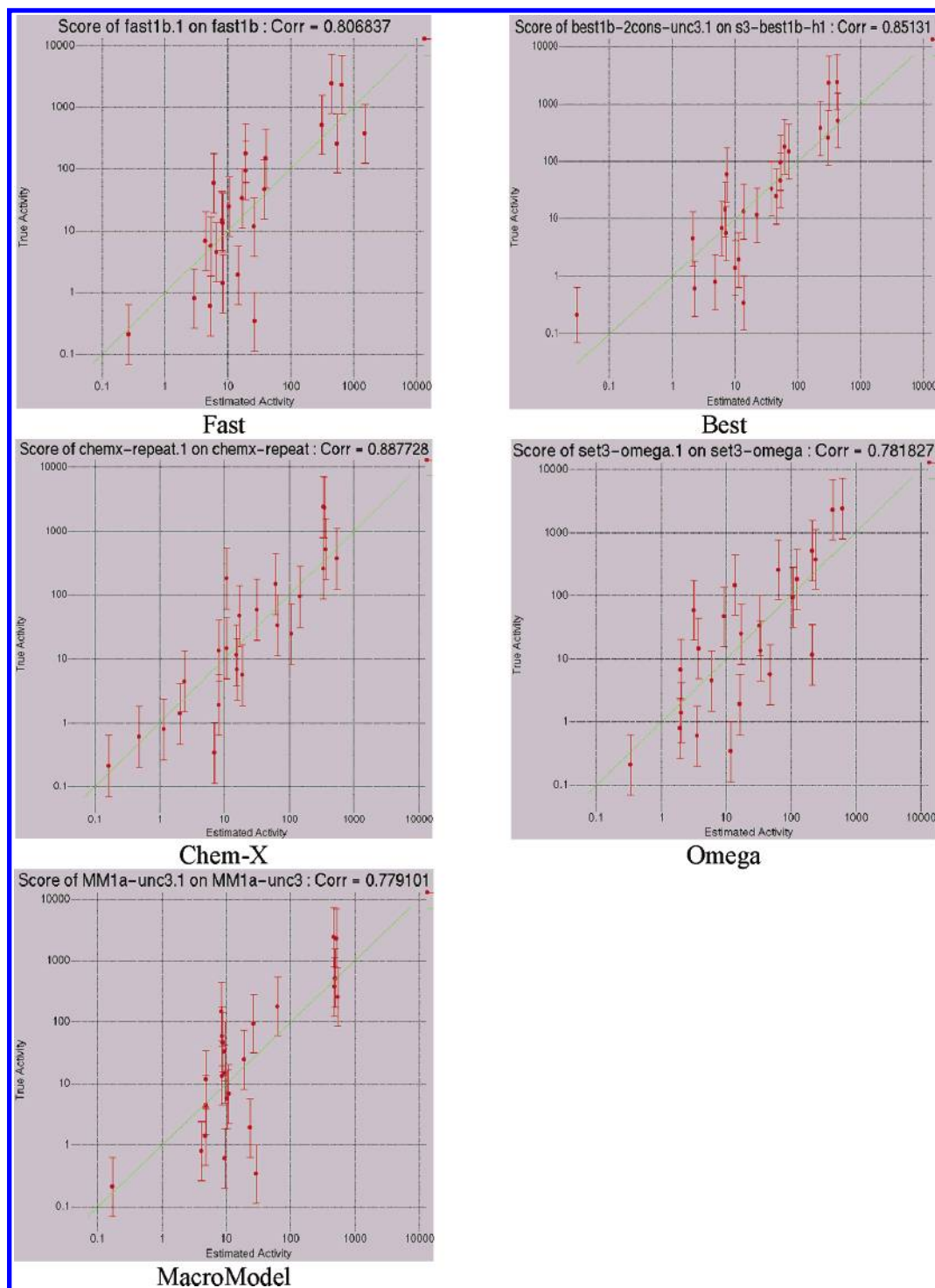


Figure 4. Predicted versus experimental values plots for the hypotheses generated for Set 2.

Table 6. Summary of the Chemical Features in the Hypotheses Generated for Set 2

CA method	features
Fast	2 HPh, 1 RA, 1 PI, 1 HBD
Best	3 HPh, 1 PI, 1 HBA
Chem-X	2 HPh, 1 RA, 1 PI, 1HBA
Omega	3 HPh, 1 PI, 1 HBA
MacroModel	3 HPh, 1 PI, 1 HBD
literature	3 HPh, 1 PI, 1 HBA

The literature hypothesis has two HBAs mapped to nitrogens of the pyrimidine (A) and pyridine (B) groups, respectively. The HPh is mapped to the methyl group of the

pyridine B, and the RA is mapped to the phenyl group, C. The Fast hypothesis is almost identical to the literature hypothesis, with the exception of the direction of the RA feature. The Best hypothesis has the HBA mapped to the pyridinyl nitrogen, B, the HPh is mapped to the methyl substituent of pyridine B and the RA is mapped to the phenyl C as for the literature model. The HBD is mapped to the 2-amino substituent of pyrimidine A. The Chem-X hypothesis has the HBA mapped to pyrimidine A, and the two HPhs are mapped to the methyl on pyridine B and the phenyl C, respectively, as for the literature model. The HBD is mapped to the amino moiety of the phenylamino, C. This hypothesis



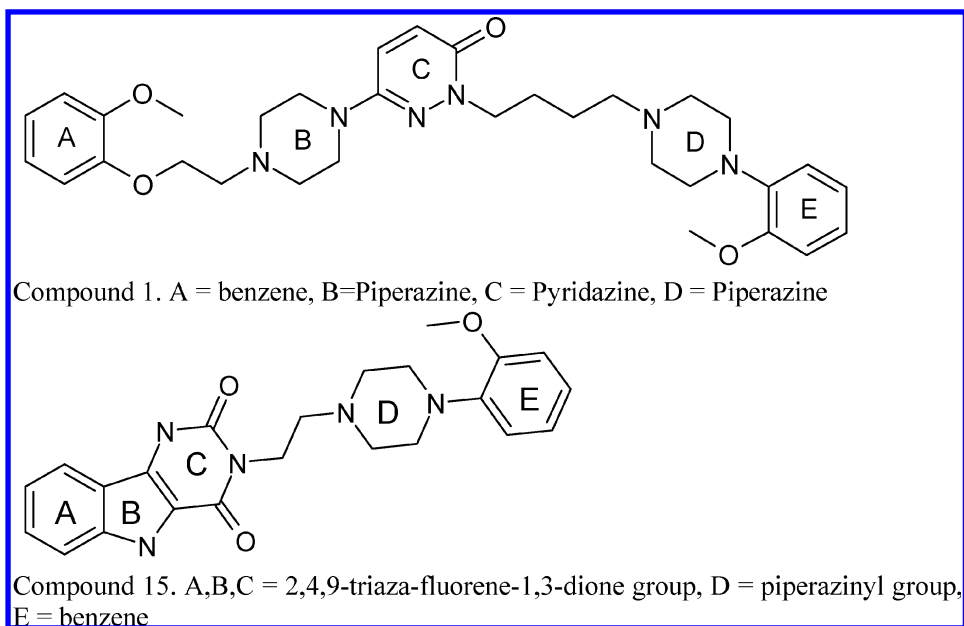


Figure 5. Compounds 1 and 15 of Set 2.

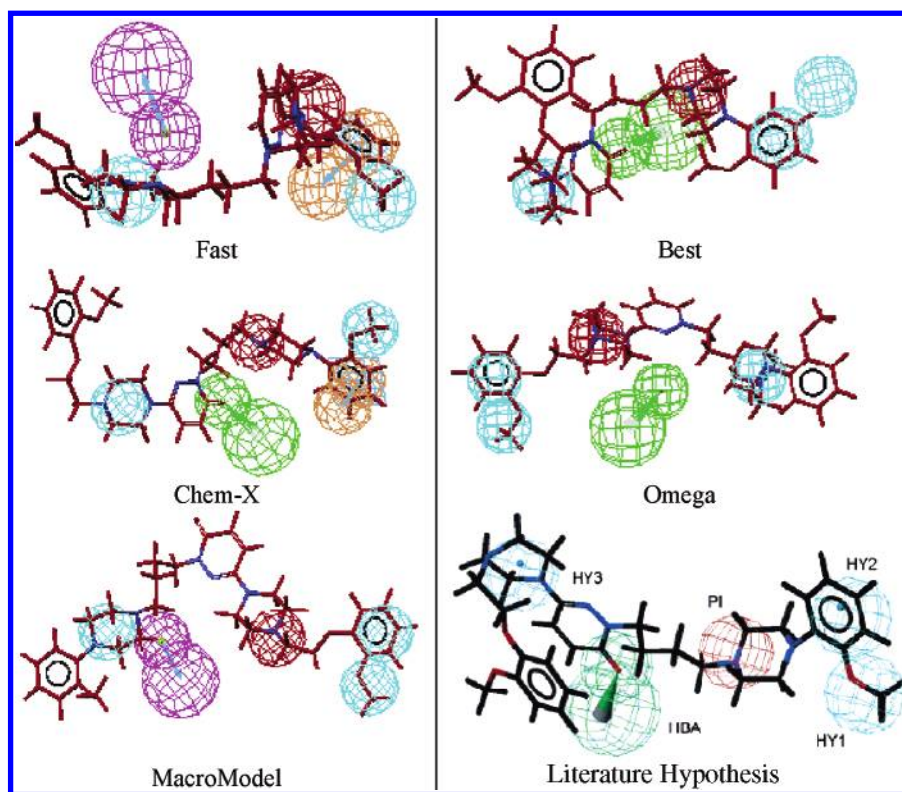


Figure 6. Mapping of the hypotheses onto compound 1 of Set 2. The bottom right hand figure is reproduced from the literature. [Reproduced with permission from *J. Med. Chem.* **2001**, *44*, 2118–2132. Copyright 2002 American Chemical Society.]

is least similar to the literature hypothesis. The Omega and MacroModel hypotheses are very similar. In each case, the HBA is mapped to the pyridine B, the HPh is mapped to the methyl substituent of pyridine B, and the RA is mapped to the phenyl C as in the literature model. The HBD is mapped to the 2-amino group of the diamine on A.

All the hypotheses map well onto compound 1 supporting the good correlation scores for all the CA sets.

All methods produced good correlation scores; however, the only hypothesis that matches the literature hypothesis for this data set is Fast, even though the literature hypothesis

was constructed using Best. In the Best hypothesis, one of the HBA groups is replaced by a HBD group.

**Set 5.** The correlation scores and costs for Set 5 are shown in Table 14. Chem-X and MacroModel gave results that are better than those reported in the literature for all three scores. The excellent Pearson's and Spearman's scores imply that both the magnitude and the relative rankings of the activities are better estimated than for the literature hypothesis. All other programs gave good Catalyst and Spearman's scores but lower Pearson's scores.

**Table 7.** Mappings of the Hypotheses onto Compounds 1 and 15 of Set 2

Mapping of Hypotheses on Compound 1						
	piperazine B	pyridazine carbonyl C	N piperazine D	benzene E	methoxy on E	other features
literature	HPh	HBA	PI	HPh	HPh	
Fast	HPh		PI	RA	HPh	HBD
Best	HPh	HBA	PI	HPh		HPh
Chem-X	HPh	HBA	PI		HPh	
Omega	HPh		PI	HPh	HPh	HBA
MacroModel	HPh		PI	HPh	HPh	HBD

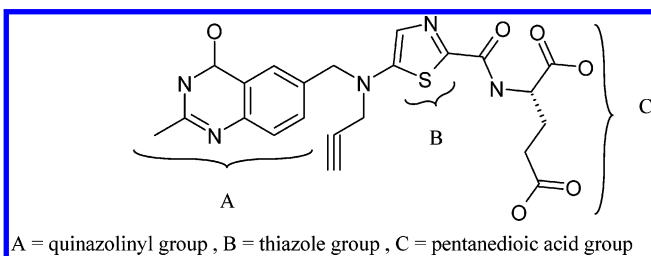
Mapping of Hypotheses on Compound 15						
	benzene A	carbonyl C	piperiziny D	benzene E	methoxy on E	other features
literature	HPh	HBA	PI	HPh	HPh	
Fast	HPh		PI	RA	HPh	HBD
Best	HPh	HBA	PI	HPh	HPh	
Chem-X	HPh	HBA	PI	RA	HPh	
Omega	HPh	HBA	PI	HPh	HPh	
MacroModel	HPh		PI	HPh	HPh	HBD

**Table 8.** Correlation Coefficient Values and Costs Obtained for Set 3

	literature	Fast	Best	Chem-X	Omega	MacroModel
Catalyst score	0.941	0.929	0.93	0.893	0.846	0.805
Pearson		0.818	0.862	0.73	0.797	0.823
Spearman		0.927	0.917	0.936	0.89	0.826
ideal cost	89.4	89.44	89.61	88.12	89.3	84.19
null cost	170.99	168.64	168.64	168.64	168.64	168.64
hypothesis cost	107.11	112.34	116.69	110.82	121.59	120.14

**Table 9.** Summary of the Chemical Features in the Hypotheses Generated for Set 3

	features
Fast	1 HPh, 3 HBA
Best	2 HPh, 2 HBA
Chem-X	1 HPh, 3 HBA
Omega	1 HPh, 3 HBA
MacroModel	1 HPh, 3 HBA
literature	1 HPh, 3 HBA

**Figure 7.** Compound 13 of Set 3.

In all cases, the difference between the ideal and null costs is around 60 bits and that between the null and the generated hypotheses is about 50–52 bits. Thus the costs again reflect the higher correlation scores seen for all the CA sets. The costs are very close to those reported in the literature.

The summary of features in the hypotheses is shown in Table 15 and the mappings of compound 14 (Figure 11) onto the hypotheses are shown in Figure 12.

The publication illustrates the mapping of a compound very similar to compound 14 on the hypothesis; the only difference is the presence of a chloro substituent in compound 14. The hypothesis has the three HBDs aligned to both the amino groups of the pyrimidinyl group and the amino group of the naphthalenyl amino group, respectively. The HPh is

mapped to the methyl substituent of the pyridinyl group. The Fast hypothesis has the HBA mapped to the nitrogen of the pyrimidinyl group, the HPh to the methyl substituent of the pyridinyl group, the HBD to the amino group of the naphthalenyl amino group and the RA to the naphthalene group. The Best hypothesis has the HBDs mapped to the amino groups of the pyrimidinyl and naphthalenyl amino groups and the HPh to the methyl substituent pyridinyl group as for the literature hypothesis. The HBA maps to the pyridinyl nitrogen. The Chem-X hypothesis has the HPh mapped to the methyl substituent of the pyridinyl group and the HBD mapped to the amino group of the naphthalenyl amino group as for the literature model. The two HBAs are mapped to the nitrogens of the pyrimidinyl and the pyridinyl groups. The Omega hypothesis has the two HPHs mapped to the methyl substituent of the pyridinyl group and the naphthalenyl group, the RA to the pyrimidinyl group and the HBD to the amino group of the naphthalenyl amino group. The MacroModel hypothesis is very similar to the Chem-X hypothesis.

Although good correlation scores were seen for all methods, it was not possible to reproduce the published hypothesis for any of them, including Fast and Best. Also, there was little consistency across the methods: in all cases at least one feature was different from the model as published and only two of the hypotheses contain the same features, those generated using Chem-X and MacroModel.

**Set 6.** All the CA programs gave excellent correlation scores for this set. The results are better than those reported in the literature. One reason could be that three of the compounds used in the original paper are drawn erroneously. The corrected structures were used in this study.

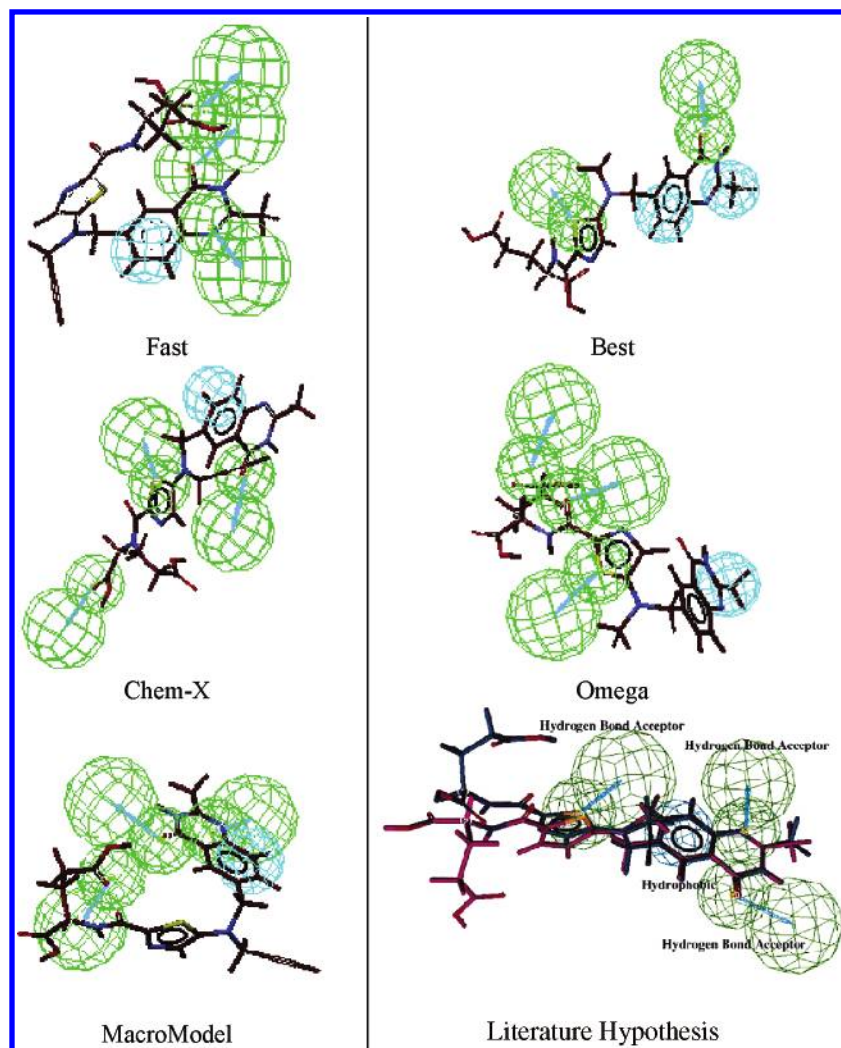


**Figure 8.** Mapping of the hypotheses onto compound 13 of Set 3. The bottom right hand figure shows the mapping of compounds 12 and 13 on hypothesis 1 given in Kim et al. [Reprinted with permission from Kim et. al. *Bioorganic & Medicinal Chemistry*, Vol. 8, 2000, Building a common feature hypothesis for thymidylate synthase inhibition. 11-17. Copyright 2000 Elsevier.]

**Table 10.** Mapping of Hypotheses onto Compound 13 of Set 3

	thiazole S	quinazolinyl carbonyl	quinazolinyl N	quinazolinyl phenyl	other
literature	HBA	HBA	HBA	HPh	
Fast		HBA	HBA	HPh	HBA carbonyl of pentadenioic
Best	HBA	HBA		HPh	HPh methyl on quinazolinyl
Chem-X	HBA	HBA		HPh	HBA carbonyl of pentadenioic
Omega	HBA			HPh	HBA carbonyl of carbonyl amino
MacroModel		HBA	HBA	HPh	HBA carbonyl of pentadenioic

**Table 11.** Correlation Coefficient Values and Costs Obtained for Set 4

	literature (Best)	Fast	Best	Chem-X	Omega	MacroModel
Catalyst Score	0.967	0.961	0.956	0.93	0.966	0.956
Pearson	0.719 <sup>a</sup>	0.617	0.877	0.96	0.706	0.706
Spearman	0.935 <sup>a</sup>	0.958	0.955	0.967	0.932	0.94
ideal cost		82.18	82.64	83.74	80.13	83.79
null cost	142.676	142.68	142.68	142.68	142.68	142.68
hypothesis cost	90.856	88.76	91.55	94.11	88.4	93.43

<sup>a</sup> Values calculated from data presented in ref 16.

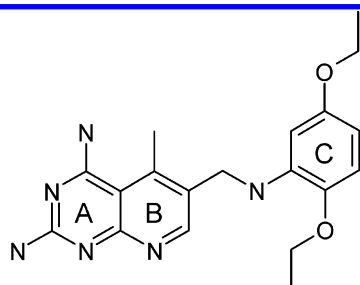
As can be seen in Table 16, MacroModel gave excellent results for Spearman's coefficient, while Chem-X gave the lowest Catalyst score although it was still good and better than that reported in the literature.

Despite the excellent scores, the difference between the ideal and null costs is only about 27 bits and that between the null hypotheses and the generated hypotheses is about 25 bits. The small differences between the ideal and null

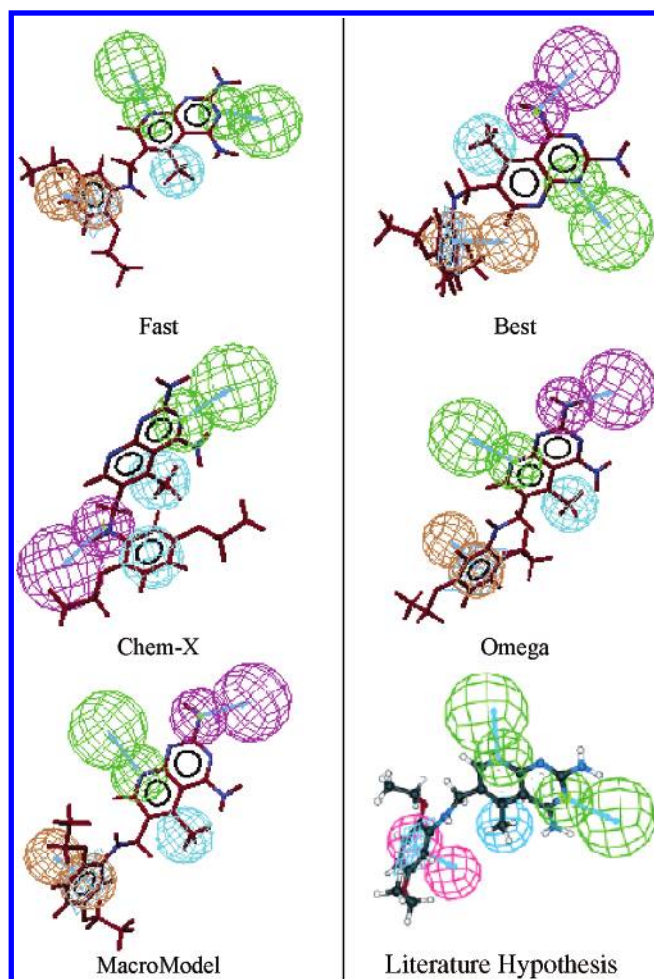


**Table 12.** Summary of the Chemical Features in the Hypotheses Generated for Set 4

	features
Fast	1 HPh, 2 HBA, 1 RA
Best	1 HPh, 1 HBA, 1 RA, 1 HBD
Chem-X	2 HPh, 1 HBA, 1 HBD
Omega	1 HPh, 1 HBA, 1 RA, 1 HBD
MacroModel	1 HPh, 1 HBA, 1 RA, 1 HBD
literature	1 HPh, 2 HBA, 1 RA



A = pyrimidinyl diamine, B = pyridinyl, C = diethoxyphenylamino

**Figure 9.** Compound 1 of Set 4.**Figure 10.** Mapping of the hypotheses onto compound 1 of Set 4. The bottom right hand figure is reproduced from the literature. [Reproduced with permission from *J. Med. Chem.* **2002**, *45*, 41–53. Copyright 2002 American Chemical Society.]

costs, as well as between the null costs and the costs of the generated hypotheses, indicate that the correlation scores and predictive abilities of the hypotheses are not significant,

despite the high correlation scores seen. A closer look at the log file revealed a configuration cost of about 18, which indicates more degrees of freedom than is recommended for hypothesis generation, giving further evidence that the generated hypotheses may not be useful.

The number and the types of chemical features of the hypotheses are given in Table 17, and the mappings of verapamil (Figure 13) on the hypotheses are shown in Figure 14.

The Fast hypothesis has the HBA mapped to the nitrogen of the nitrile group, both the HPhs are mapped to one of the methoxy groups of both the dimethoxy phenyl groups, and the RA is mapped to the 2-dimethoxy phenyl group. The Best, Chem-X and Omega hypotheses show a similar mapping. The MacroModel hypothesis has the HBA mapped to the nitrile group, the HPh to the methoxy substituent of the 2-dimethoxyphenyl group and both the RAs to the phenyl moieties of both the dimethoxy phenyl groups. Since all the hypotheses map to the compound in the same way, they yield similar results and compare well.

In summary, the literature model was reproduced; however, the poor cost value and high configuration costs cast doubt on the statistical validity of the models.

## DISCUSSION

The aim of this work was to compare the performance of the five different conformational analysis methods for the generation of Catalyst pharmacophore hypotheses for high quality data sets for which Catalysts models had been published. Hypotheses were generated for each of the selected data sets, and the performance across the different conformational analysis methods was compared using both quantitative and qualitative measures. The results were also compared with the literature hypotheses.

There are three major conclusions from this work. First, the 'fast' conformational analysis programs, in particular Chem-X, perform as well as the more computationally expensive tools such as Best; second, we found it difficult to reproduce the literature hypotheses, even at the level of the number and type of the pharmacophore features used; and third, the consistency of the hypotheses generated using different conformational analysis methods is poor, especially for some of the data sets. These issues are discussed in more detail below.

Table 18 summarizes the correlation scores for all conformational analysis methods across all data sets. In general, all of the programs performed well based on these measures, with the exception of Set 3 for Chem-X, Omega and MacroModel. Chem-X and Best outperformed the others in the case of Set 2. However, despite the generally good performance given according to these measures, there is little consistency in the hypotheses generated for some of the data sets as discussed below.

It should be noted that the measures applied here are measures of internal correlation and do not indicate the extent to which the hypotheses can be used for prediction. A comparison of the predictive abilities of the models using an independent test set would provide an additional evaluation criterion. This was not done here, since the principal aim of the study was to compare results with the literature

**Table 13.** Mapping of Hypotheses onto Compound 1 of Set 4

	pyrimidine A	pyridine B	methyl on B	benzene C	other
literature	HBA	HBA	HPh	RA	
Fast	HBA	HBA	HPh	RA	
Best		HBA	HPh	RA	HBD (2-amino on A)
Chem-X	HBA		HPh	HPh	HBD (N on C)
Omega		HBA	HPh	RA	HBD (2-amino on A)
MacroModel		HBA	HPh	RA	HBD (2-amino on A)

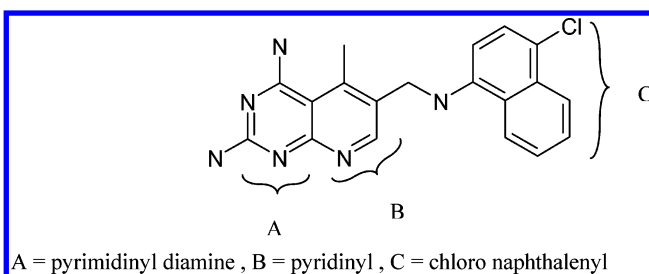
**Table 14.** Correlation Coefficient Values and Costs Obtained for Set 5

	literature (Best)	Fast	Best	Chem-X	Omega	MacroModel
Catalyst score	0.973	0.975	0.954	0.98	0.957	0.983
Pearson	0.847 <sup>a</sup>	0.68	0.791	0.989	0.464	0.985
Spearman	0.874 <sup>a</sup>	0.938	0.893	0.892	0.919	0.937
ideal cost	83.088	82.56	83.07	84.68	81.32	84.34
null cost	140.098	140.1	140.1	140.1	140.1	140.1
hypothesis cost	88.167	88.21	90.61	88.28	88.94	88.17

<sup>a</sup> Values calculated from data presented in ref 16.

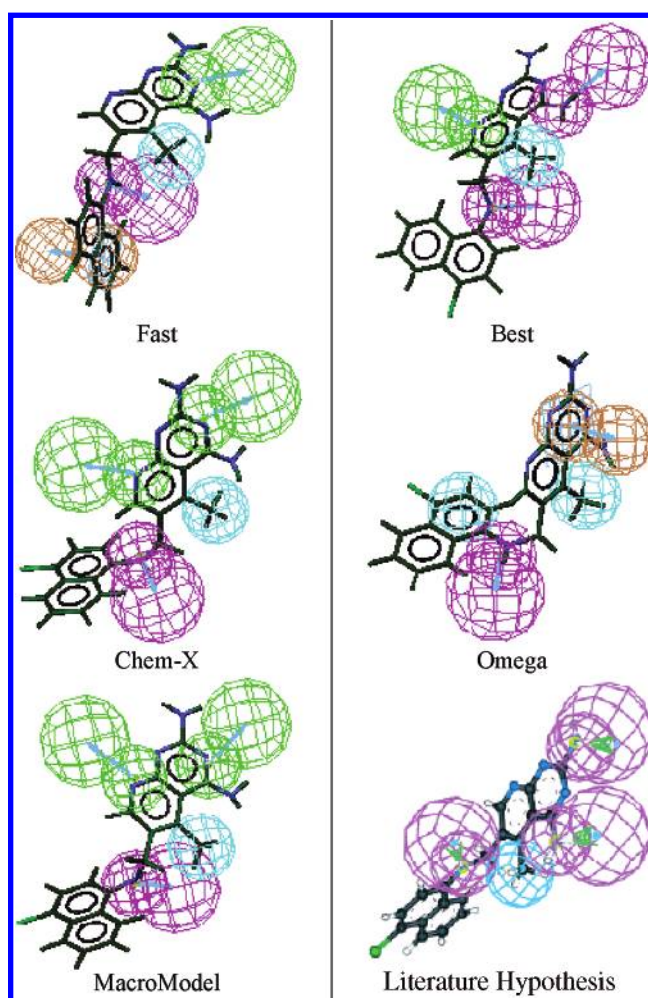
**Table 15.** Summary of the Chemical Features in the Hypotheses Generated for Set 5

	features
Fast	1 HPh, 1 HBA, 1 RA, 1HBD
Best	1 HPh, 1 HBA, 2 HBD
Chem-X	1 HPh, 2 HBA, 1 HBD
Omega	2 HPh, 1 RA, 1 HBD
MacroModel	1 HPh, 2 HBA, 1 HBD
literature	1 HPh, 3 HBD

**Figure 11.** Compound 14 of Set 5.

hypotheses. However, the use of an independent test set is strongly recommended as part of the publication template for pharmacophore models suggested below, given the variation in pharmacophore models observed in this study.

The qualitative comparison revealed inconsistencies in the hypotheses generated using the different conformer sets. We were expecting to see differences in the geometry of the hypotheses, as the bioactive conformation is often under-determined, except when the data set contains some very rigid ligands that also have high affinity. However, we were hoping to observe greater consistency in the number and type of the pharmacophore features in the hypotheses than was observed. For Set 1, since it is not known which of the top 10 models was selected as the literature hypothesis, the hypothesis in the top 10 that was closest to the literature hypothesis was chosen in each case. The fourth-ranked Best model did correspond with the published model. The Chem-X model (hypothesis at rank 5) contained the same features as the literature model; however, the mapping to compounds in the training set differed. Both the MacroModel (hypothesis at rank 1) and Fast (hypothesis at rank 5) models missed the PI feature, and the Omega model (hypothesis at rank 5) exchanged an HBA for a Hydrophobic feature. For Set 2, the Best and Omega hypotheses consist of the same

**Figure 12.** Mapping of compound 14 to the hypotheses. The bottom right hand figure is reproduced from the literature and shows the mapping of compound 62, which is similar to compound 14, on hypothesis 1. [Reproduced with permission from *J. Med. Chem.* 2002, 45, 41–53. Copyright 2002 American Chemical Society.]

features as the literature model; however, in both cases the spatial arrangement of the features was different. The Fast and MacroModel hypotheses both exchanged a HBD feature for HBA. For Set 3, all methods except Best produced hypotheses that contain the same features as the literature model; however, in all cases the spatial arrangement of the

**Table 16.** Correlation Coefficient Values and Costs for the First Four Hypotheses for Set 6

	literature <sup>a</sup>	Fast	Best	Chem-X	Omega	MacroModel
Catalyst score		0.983	0.980	0.974	0.977	0.979
Pearson		0.935	0.934	0.898	0.968	0.945
Spearman	0.87	0.985	0.976	0.953	0.962	0.994
R <sup>2</sup>	0.55	0.874	0.874	0.806	0.937	0.893
ideal cost		73.46	73.14	73.42	72.97	72.97
null cost	101.1	101.15	101.15	101.15	101.15	101.15
hypothesis cost	75.2	75.2	75.01	76.24	75.38	75.24

<sup>a</sup> Data given are for the Digoxin Transport Model.**Table 17.** Summary of the Chemical Features in the Hypotheses Generated for Set 6

	features
Fast	2 HPh, 1 HBA, 1 RA
Best	2 HPh, 1 HBA, 1 RA
Chem-X	2 HPh, 1 HBA, 1 RA
Omega	2 HPh, 1 HBA, 1 RA
MacroModel	1 HPh, 1 HBA, 2 RA
literature	2 HPh, 1 HBA, 1 RA

features differs from the literature model as does the mapping of the features onto the example compound. For Set 4, only the Fast hypothesis matched the published model, yet in the publication, the hypothesis was constructed using Best. In the Best hypothesis one of the HBA groups was replaced by a HBD group. It was not possible to reproduce the published hypothesis for Set 5, with either Fast or Best: in fact, none of the hypotheses matched the published hypothesis. In all cases at least one feature was different from the model as published, and only two of the hypotheses contain the same features, those generated using Chem-X and MacroModel. For Set 6, the literature model was reproduced; however, the poor cost value and high configuration cost cast doubt on the statistical validity of the models.

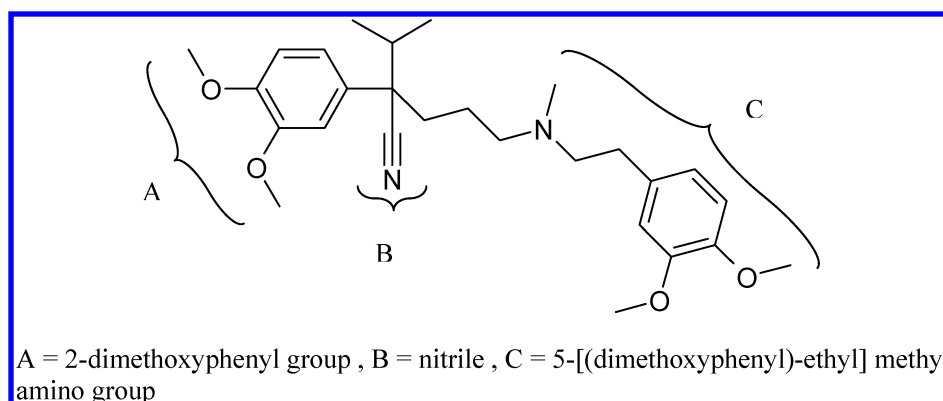
It may be that changes made to the global settings of the Catalyst program have not been reported in the publications, and this may account for the failure to reproduce the literature models. Catalyst allows various settings and parameters to be altered from their default values. For example, new features or fragments can be defined, or default features can be modified to suit the needs of the experiment. In particular the feature dictionary and property dictionary can be modified by making changes to the features or to the functional behavior of certain fragments. There are many other parameters that can be varied during a hypothesis generation run. Changes can be made globally at the level of Catalyst system files that will affect all the subsequent Catalyst runs so that

users may not be aware that they are using nondefault values. Changes may also be made locally by users, which can affect just the current session. This indicates the need for the exact settings for hypothesis generation to be outlined in full, and, in particular, changes to the standard dictionary must be described explicitly, otherwise, replication of the model may not be possible.

There may also be differences due to different versions of Catalyst being used. To avoid this, it has been suggested that, where possible, the version of Catalyst that was originally used to build the model should be used. However, this is not always feasible due to incompatibilities with other changes in the operating system. In addition, a pharmacophore is meant to reflect the true drug-receptor interaction, so we would hope that the hypotheses would remain qualitatively the same across versions of Catalyst.

There are also many parameters that control the conformational analysis methods Fast and Best (for example, the *cis/trans* ratio in peptides), and the behavior of the algorithms has changed markedly across versions (for example, the treatment of axial and equatorial preferences in aliphatic nitrogen heterocycles such as piperidines). A final issue to arise is that different conformations can be generated depending on the hardware (chip set) and operating system used, due to rounding errors. Furthermore, others have demonstrated the dependence of the conformers generated on the initial starting structure.<sup>24</sup> Here, Corina was used to generate the initial structure, while some of the publications may have used a different method. Best and Fast will also generate their own starting conformations.

Our limited sets of observations of the efficiency of the various conformational analysis methods are in line with the more complete study by Boström.<sup>7</sup> We conclude that the more computationally expensive programs do not seem to offer any advantages over the quick rule-based methods for this application, considering the quality of pharmacophore

**Figure 13.** Verapamil from Set 6.



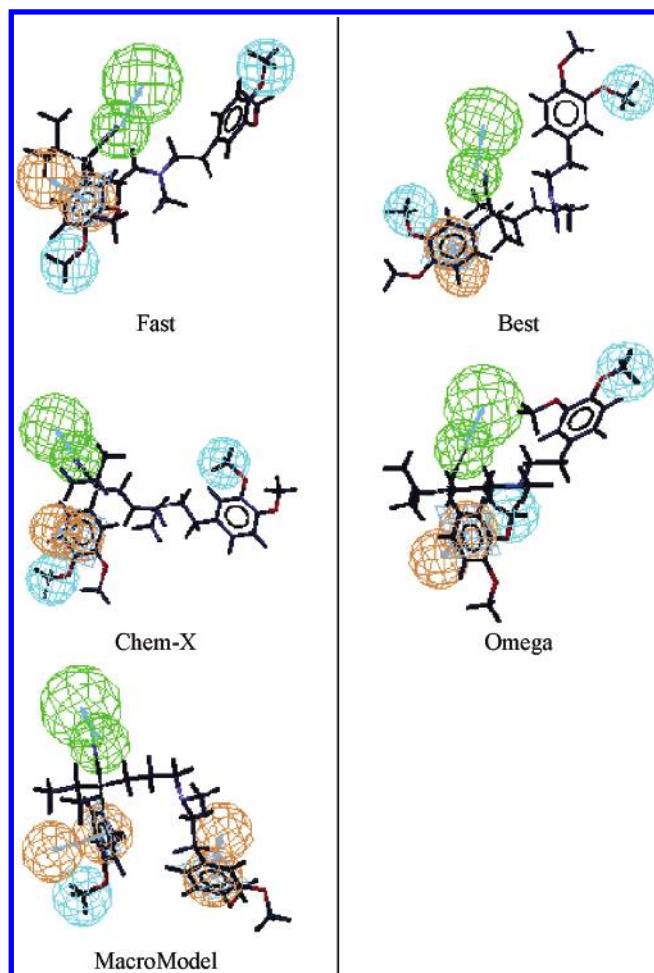


**Figure 14.** Mapping of Verapamil onto the hypotheses for Set 6.

**Table 18.** Catalyst Scores for the First Hypothesis for Each Set

Catalyst score	Fast	Best	Chem-X	Omega	MacroModel
Set 1	0.892	0.964	0.978	0.942	0.955
Set 2	0.807	0.851	0.888	0.782	0.779
Set 3	0.929	0.93	0.893	0.846	0.805
Set 4	0.961	0.956	0.93	0.966	0.956
Set 5	0.975	0.954	0.98	0.957	0.983
Set 6	0.983	0.98	0.974	0.977	0.979

models produced. Both Chem-X and Omega produced acceptable results for pharmacophore generation in a fraction of the time required for MacroModel or Best. If efficiency is taken into account as well as effectiveness, then Chem-X seemed to perform most satisfactorily since it gave better results and took the second least time of all the programs. The more expensive CA methods may not lead to better hypotheses, as the limiting factor may lie elsewhere, for example, in the quality of the biological data or in the space explored by the structures in the data set.

As a consequence of the difficulties encountered in this work, we propose the use of a general template for publication of pharmacophore hypotheses generated using the Catalyst methodology (see Table 19) to improve the reproducibility of hypotheses. Despite the feeling that many of the requirements of the template are obvious, our research has revealed that even the most basic experimental data are taken for granted and not specified. Finally, the observed variations in the hypotheses can be seen in a positive light. The differences arising from the CA method used could also

**Table 19.** Hypothesis Specification Requirements<sup>a</sup>

	requirement
1	Complete specification of all stereochemistry and how chiral molecules are treated
2	Catalyst version and CPU platform
3	Contents of the Catalyst parameter file must be declared to be standard, or any changes described.
4	Complete details of the conformational analysis technique used including the technique for initial conformer generation, energy cutoff, the number of conformers generated, issues with stereochemistry, any other preferences.
5	The uncertainty value must be given.
6	Any feature changes to the standard dictionary must be specified.
7	The choice and number of features used in the hypothesis construction, i.e., 2*HBA and 5*PI.
8	Settings for hypothesis generation in Catalyst, including weight variation, variable tolerance, spacing, MinPoints, MinSubsetPoints, Mapping coefficient, Feature Misses, Superposition error, check superposition tolerance factor, etc.
9	The source of all activity data must be specified accurately.
10	The number, type, weighting, tolerance and separation of features in a resulting hypothesis should be given.
11	The predicted activity values.
12	An independent test set should be used to assess the model.

<sup>a</sup> Ideally the Catalyst parameter file “.Catalyst” should be made available as Supporting Information.

highlight where the structure–activity relationship is under-determined, and where further analogues should be made. This again emphasizes the need for a good independent test set.

## CONCLUSIONS

Six training sets from the literature have been used to construct Catalyst hypotheses using five conformational analysis techniques (Catalyst/Fast, Catalyst/Best, Chem-X, Omega and MacroModel). It has been shown that fast conformation generation tools perform as well as expensive tools, in terms of the quality of the pharmacophore models produced. We found conformers generated using Best and Chem-X produce a set of quality hypotheses that are as good as or better than those reported in the literature; however, the Chem-X protocol is much faster. We found it difficult to reproduce the literature hypotheses with accuracy. From the six sets examined, only in the case of three sets (1, 2 and 6) have we been able to produce a Catalyst/Best hypothesis that is close to the original publication. We discovered that some of the essential details required for hypothesis generation were missing, and default values had to be used. Based on these findings, we propose a template for Catalyst based literature publications to facilitate the replication of pharmacophore models.

## ACKNOWLEDGMENT

The authors gratefully acknowledge discussions and helpful advice and insights from Drs. Jon Erickson, Thierry Langer, Tien Luu and Ulf Norinder.

**Supporting Information Available:** Structures and activity tables (sets 1–6). This material is available free of charge via the Internet at <http://pubs.acs.org>.

## REFERENCES AND NOTES

- (1) Farmer, P. S.; Ariens, E. J. Speculations on the Design of Nonpeptidic Peptidomimetics. *Trends Pharm. Sci.* **1982**, 3(9), 362–5.

- (2) *Pharmacophore Perception, Development, and Use in Drug Design*; Güner, O. F., Ed.; California, USA: International University Line, 2000.
- (3) Barnum, D.; Greene, J.; Smellie, A.; Sprague, P. Identification of Common Functional Configurations Among Molecules. *J. Chem. Inf. Comput. Sci.* **1996**, *36*, 563–571.
- (4) Jones, G.; Willett, P.; Glen, R. C. A Genetic Algorithm for Flexible Molecular Overlay and Pharmacophore Elucidation. *J. Comput.-Aided Mol. Des.* **1995**, *9*, 532–549.
- (5) Martin, Y. C.; Bures, M. G.; Danaher, E. A.; DeLazzer, J.; Lico, I.; Pavlik, P. A. A Fast New Approach to Pharmacophore Mapping and its Application to Dopaminergic and Benzodiazepine Agonists. *J. Comput.-Aided Mol. Des.* **1993**, *7*, 83–102.
- (6) Catalyst, Accelrys, 9685 North Scranton Road, San Diego, CA 92121, USA. <http://www.accelrys.com/>.
- (7) Boström, J. Reproducing the Conformations of Protein-Bound Ligands: A Critical Evaluation of Several Popular Conformational Searching Tools. *J. Comput.-Aided Mol. Des.* **2001**, *15*, 1137–1152.
- (8) Diller, D. J.; Merz, K. M., Jr. Can We Separate Active From Inactive Conformations? *J. Comput.-Aided Mol. Des.* **2002**, *16*, 105–112.
- (9) Daveu, C.; Bureau, R.; Baglin, I.; Prunier, H.; Lancelot, J. C.; Rault, S. Definition of a Pharmacophore for Partial Agonists of Serotonin 5-HT<sub>3</sub> Receptors. *J. Chem. Inf. Comput. Sci.* **1999**, *39*, 362–369.
- (10) Leach, A. R. *Molecular Modelling. Principles and Applications*; Pearson Education Limited: Harlow, 2001.
- (11) Boström, J.; Greenwood, J. R.; Gottfries, J. Assessing the Performance of OMEGA with Respect to Retrieving Bioactive Conformations. *J. Mol. Graphics Modell.* **2003**, *5*, 449–462.
- (12) Kurogi, Y.; Güner, O. F. Pharmacophore Modeling and Three-dimensional Database Searching for Drug Design Using Catalyst. *Curr. Med. Chem.* **2001**, *8*, 1035–1055.
- (13) Bureau, R.; Daveu, C.; Lemaitre, S.; Dauphin, F.; Landelle, H.; Lancelot, J.-C.; Rault, S. Molecular Design Based on 3D-Pharmacophore. Application to 5-HT<sub>4</sub> Receptor. *J. Chem. Inf. Comput. Sci.* **2002**, *42*, 962–967.
- (14) Barbaro, R.; Betti, L.; Botta, M.; Corelli, F.; Giannaccini, G.; Maccari, L.; Manetti, F.; Strappaghetta, G.; Corsano, S. Synthesis, Biological Evaluation, and Pharmacophore Generation of New Pyridazinone Derivatives with Affinity toward  $\alpha_1$ - and  $\alpha_2$ -Adrenoceptors. *J. Med. Chem.* **2001**, *44*, 2118–2132.
- (15) Kim, S. G.; Yoon, C. J.; Kin, S. H.; Cho, Y. J.; Kang, D. I. Building a Common Feature Hypothesis for Thymidylate Synthase Inhibition. *Bioorg. Med. Chem.* **2000**, *8*, 11–17.
- (16) Debnath, A. K. Pharmacophore Mapping of a Series of 2,4-Diamino-5-deazapteridine Inhibitors of *Mycobacterium avium* Complex Dihydrofolate Reductase. *J. Med. Chem.* **2002**, *45*, 41–53.
- (17) Ekins, S.; Kim, R. B.; Leake, B. F.; Dantzig, A. H.; Schuetz, E. G.; Lan, L.-B.; Yasuda, K.; Shepard, R. L.; Winter, M. A.; Schuetz, J. D.; Wikel, J. H.; Wrighton, S. A. Application of Three-Dimensional Quantitative Structure–Activity Relationships of P-Glycoprotein Inhibitors and Substrates. *Mol. Pharmacol.* **2002**, *61*, 974–981.
- (18) Corina, Molecular Networks GmbH, Computerchemie Nögelsbachstrasse 25, 91052 Erlangen, Germany.
- (19) ConFirm, Available at <http://www.accelrys.com/catalyst/confirm.html>.
- (20) Smellie, A.; Teig, S. L.; Towbin, P. Poling: Promoting Conformational Variation. *J. Comput. Chem.* **1995**, *16*, 171–187.
- (21) Mason, J. S.; Morize, I.; Menard, P. R.; Cheney, D. L.; Hulme, C.; Labaudiniere, R. F. New 4-Point Pharmacophore Method for Molecular Similarity and Diversity Applications: Overview of the Method and Applications, Including a Novel Approach to the Design of Combinatorial Libraries Containing Privileged Substructures. *J. Med. Chem.* **1999**, *42*, 3251–3264.
- (22) OMEGA, OpenEye Scientific Software, 3600 Cerrillos Rd., Suite 1107 Santa Fe, NM 87507, USA.
- (23) MacroModel, Schrodinger Inc., 1500 S.W. First Avenue, Suite 1180, Portland, OR 97201, USA.
- (24) Van Geerestein, V. J.; Verwer, P. Quality assessment of built 3D structures in context of flexible searching. Book of Abstracts, 211th ACS National Meeting, New Orleans, LA, March 24–28, 1996.

CI049731Z